Reduced buckling in one dimension versus two dimensions of a compressively strained film on a compliant substrate

R. L. Peterson[a)]
Princeton Institute for the Science and Technology of Materials, Princeton University, Princeton, New Jersey 08540 and Department of Electrical Engineering, Princeton University, Princeton, New Jersey 08544

K. D. Hobart and F. J. Kub
Naval Research Laboratory, Washington, DC 20375

H. Yin and J. C. Sturm
Princeton Institute for the Science and Technology of Materials, Princeton University, Princeton, New Jersey 08540 and Department of Electrical Engineering, Princeton University, Princeton, New Jersey 08544

Compliant substrates are useful for manipulating the strain state of thin films. However the compliant layer may permit undesirable roughening (buckling) of a compressively strained film. In this work, we quantitatively compare two-dimensional and one-dimensional buckling in thin silicon-germanium films under biaxial and uniaxial compressive stresses, respectively. For the same strain level, films with one-dimensional stress and thus one-dimensional buckling exhibit slower buckling and lower final steady state buckling amplitude, which makes them technologically advantageous compared to biaxially strained films, which exhibit two-dimensional buckling. The results are explained through modeling. © *2006 American Institute of Physics.*
[DOI: 10.1063/1.2204456]

In recent work, compressively strained SiGe films are transferred to a silicon wafer coated with borophosphorosilicate glass (BPSG), which functions as a compliant substrate. The SiGe layer is patterned into islands. When heated to about 750 °C, the BPSG softens and allows the SiGe to laterally expand and relax, enabling SiGe relaxed layers (and strained silicon in two-layer structures) in a process that does not require misfit dislocations.[1,2] Most recently, by using rectangular islands, which allow relaxation in one direction but not in the other, SiGe with uniaxial stress and uniaxially strained silicon films with uniform strain over relatively large areas have been realized.[3] A critical limiting mechanism for this process is that the islands tend to buckle during annealing to relieve stress, in addition to their lateral expansion (Fig. 1 inset).[1,2,4,5] In this work, we experimentally and theoretically examine this buckling effect in SiGe films with uniaxial stress and, most importantly, find that significantly less buckling occurs in the uniaxial compared to the conventional biaxial stress case.

Initially a 30 nm $Si_{0.7}Ge_{0.3}$ layer with a compressive strain ε_0 of −1.2% is grown pseudomorphically on a sacrificial bulk (001) silicon wafer. By wafer bonding and Smart-Cut™ the SiGe is transferred with full strain onto a silicon handle wafer coated with 235 nm BPSG (4.4% B and 4.1% P by weight). The SiGe layer is patterned into islands and annealed at 750 °C. The type of stress that results is determined by island shape. For square islands, the initial in-plane stress $\sigma_{biaxial}$ and strain $\varepsilon_{biaxial} = \varepsilon_0$ are biaxially symmetric and related by $\sigma_{biaxial} = E\varepsilon_{biaxial}/(1-\nu) = -2.0$ GPa, where $E = 121$ GPa is Young's modulus and $\nu = 0.28$ is Poisson's ratio for $Si_{0.7}Ge_{0.3}$ in the $\langle 100 \rangle$ direction.[6,7] As the anneal pro-

ceeds, the SiGe stress at the island center relaxes with a lateral relaxation time constant proportional to L^2, where L is the island edge length.[2,8] For rectangular islands, the L^2 dependence of relaxation time is exploited to generate uniaxial stress.[3] A rectangular island quickly relaxes in the short direction to zero stress ($\sigma_{short} = 0$), while in the island long direction strain changes much more slowly and thus is effectively pinned to its initial value ($\varepsilon_{long} = \varepsilon_0$). From Hooke's law, one can calculate stress in the long direction as $\sigma_{uniaxial} = E\varepsilon_0 = -1.5$ GPa. The biaxial stress $\sigma_{biaxial}$ is greater than uniaxial stress $\sigma_{uniaxial}$ due to the Poisson effect of the nonzero compressive stress in the perpendicular in-plane direction. So after a brief relaxation anneal, a narrow rectan-
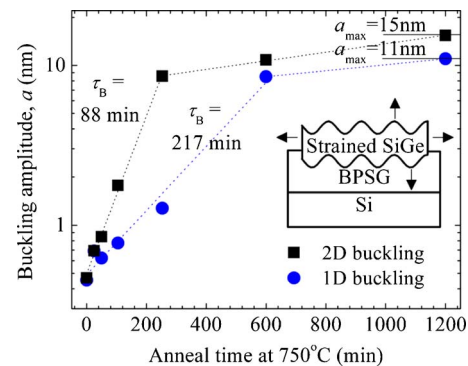

FIG. 1. (Color online) Buckling amplitude, measured by AFM as rms surface roughness, versus anneal time at 750 °C, for 1D (blue circles) and 2D (black squares) buckling. Dotted lines show the exponential growth of buckling using extracted values of τ_B. Short solid lines indicate the maximum observed buckling amplitude a_{max}. The inset schematic shows a SiGe film, initially flat, releasing its stress upon high temperature anneal via two simultaneous, competing mechanisms indicated by the arrows: lateral expansion to generate a flat, relaxed film; and buckling (vertical expansion) to create a rough surface.

[a)]Present address: Cavendish Laboratory, University of Cambridge, Cambridge CB3 0HE, UK; electronic mail: rlp38@cam.ac.uk
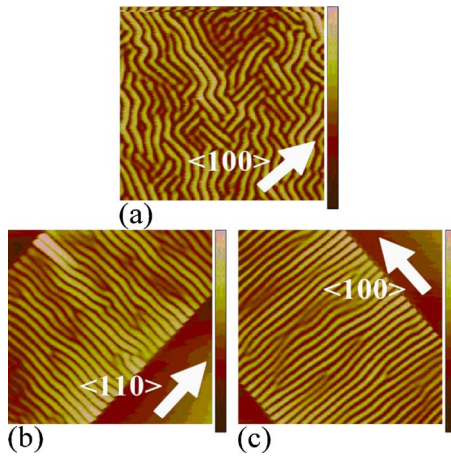
FIG. 2. (Color online) AFM images of SiGe on BPSG islands (Fig. 1 inset): (a) 2D buckling at the center of a square island, 150×150 μm^2; (b) and (c) 1D buckling at the center of rectangular islands, 20×150 μm^2, aligned to the $\langle 110 \rangle$ and $\langle 100 \rangle$ crystal directions, as indicated, after a 20 h anneal at 750 °C. The AFM scan size is 25×25 μm^2 and the z-axis scale is 70 nm.

TABLE I. Summary of measured and modeled buckling parameters for 2D and 1D buckling. The values predicted by modeling are in parentheses.

Buckling parameter	2D	1D	Ratio: 1D/2D
Time constant τ_B	88 min (88 min)	217 min (172 min)	2.5 (2.0)
Wavelength λ	0.91 μm (0.62 μm)	0.94 μm (0.70 μm)	1.0 (1.1)
Amplitude a_{max}	15 nm (26 nm)	11 nm (22 nm)	0.73 (0.85)

gular island of SiGe film will have uniaxial in-plane stress, while the center of a large square island will maintain its initial, larger biaxial stress.

In addition to this desired lateral expansion mode there is an undesirable buckling mode[1,2] which competes with lateral expansion (Fig. 1 inset). Buckling is driven by stress; as a film buckles, it relieves its stress. If stress in the plane of the film is biaxially symmetric (as at the center of large square islands), buckles can form in both in-plane dimensions [Fig. 2(a)] before lateral relaxation occurs. Initially the buckling amplitude a, measured by atomic force microscopy (AFM), grows exponentially with time t according to $a(t) = a_0 \exp(t/\tau_B)$, where τ_B is the buckling time constant.[4] At the center of large (> 100 μm edge length) islands, the observed initial buckling growth is indeed exponential with time (Fig. 1) with a time constant τ_B of 88 min. Upon further annealing, buckling effectively stabilizes. The buckling saturates because a majority of the initial film stress has been relieved by buckling, reducing the driving force for buckling. The maximum buckling amplitude a_{max}, observed after a 20 h anneal at 750 °C, is 15 nm. The buckling wavelength λ is approximately 0.91 μm. As observed previously[1,5] and in Fig. 2(a), the buckles are aligned to the $\langle 100 \rangle$ crystal directions. This alignment occurs because the buckling rate ($1/\tau_B$) is fastest in this direction; the buckling time constant τ_B varies with crystal direction through Young's modulus E and Poisson's ratio ν.[5–7] Using the equations of Ref. 4, and a BPSG viscosity of 5.8×10^{11} N s m^{-2}, one can calculate the dependence of τ_B on the crystal direction in the (001) plane: τ_B has a minimum value of 88 min in the $\langle 100 \rangle$ directions, and a maximum value of 107 min in the $\langle 110 \rangle$ directions. Thus, the film buckles most quickly in the $\langle 100 \rangle$ directions.

When the SiGe layer is patterned into a rectangular island and annealed, the island's short direction rapidly laterally relaxes until its stress is zero, while the island's long direction remains fully strained.[3] One-dimensional (1D) buckling is measured at the center of rectangular islands sized 20×150 μm^2. The island size is chosen such that in the short direction the island center relaxes to zero stress after annealing for less than 2 h at 750 °C, quickly creating a state of uniaxial stress under which 1D buckling can occur.[9] Figures 2(b) and 2(c) show AFM images of buckled

rectangular islands with edges aligned to $\langle 110 \rangle$ and $\langle 100 \rangle$. In both cases, buckling occurs along the long direction, *regardless of island* orientation, confirming that the rectangle orientation (and thus the direction of high stress) determines the direction of 1D buckling.

In Fig. 1, the 1D buckling amplitude at the center of rectangular islands with edges aligned to the $\langle 100 \rangle$ crystal direction in the (001) surface plane of the film is plotted versus anneal time. The 1D buckling amplitude initially grows exponentially and later stabilizes, as in the two-dimensional (2D) buckling case. For 1D buckling the extracted buckling time constant, 217 min, is about 2.5 times longer than τ_B for 2D buckling (88 min).

The longer buckling time constant occurs because in the 1D case the stress in the direction of buckling $\sigma_{uniaxial}$ is much lower than that in the biaxial case $\sigma_{biaxial}$, as described earlier. The lower magnitude of stress provides less of a driving force for buckling, and thus buckling occurs more slowly in the uniaxial case, despite the fact that in both cases the strain in the direction of buckling is equal to the original ε_0 of the SiGe. To quantify this difference, we look to existing 2D buckling theories.[4] The buckling rate, referred to in Ref. 4 as s_1, is calculated for all possible wavelengths (through buckling wave numbers k, where $k = 2\pi/\lambda$). The maximum buckling rate is determined numerically and is assumed to dominate buckling so that $\tau_B = (s_{1,max})^{-1}$. The wave number k_m, at which this maximum occurs, corresponds to the expected buckling wavelength λ_m. In Ref. 4, 2D buckling is modeled as a one-dimensional process (for analytical ease), but the stresses parallel and normal to the buckles are assumed to be identical and equal to $\sigma_{biaxial}$. To model 1D buckles, we instead assume zero stress normal to the buckles. The only resulting change is to Eq. (29) of Ref. 4, which becomes

$$\alpha = \frac{E k h_{SiGe}}{24 \eta (1 - \nu^2)} \left[-12\sigma\left(\frac{1 - \nu^2}{E}\right) - (k h_{SiGe})^2 \right] \gamma_{11}, \quad (1)$$

where h_{SiGe} is the film thickness, η is the BPSG viscosity (5.8×10^{11} N s m^{-2} at 750 °C, determined by fitting the 2D buckling time constant model of Ref. 4 to measured data), and γ_{11}, defined in Eq. (11) of Ref. 4, is a function of k and the BPSG thickness. The variable σ represents the stress in the direction of buckling, $\sigma_{uniaxial}$ or $\sigma_{biaxial}$. The value of α is used to calculate s_1 and thus τ_B (see Ref. 4); in general as α decreases, τ_B increases.

Because $|\sigma_{uniaxial}| < |\sigma_{biaxial}|$, these calculations predict that τ_B will approximately double from 88 min for 2D buckles to 172 min for 1D buckles (2.0 times). The experimental results indicate a similarly large increase of 2.5 times (Table I). The larger buckling time constant of 1D buckling com-
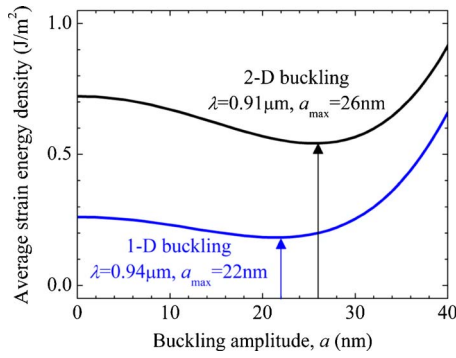
FIG. 3. (Color online) Average strain energy density of 1D and 2D buckled films vs buckling amplitude. The energy curves are plotted for the measured buckling wavelengths, as indicated. Arrows indicate the buckling amplitude at the minimum energy equilibrium state of the film, a_{max}.

pared to 2D buckling can thus be attributed to the lower value of uniaxial stress compared to biaxial stress for the same film structure and is technologically quite advantageous.

The maximum buckling amplitude a_{max}, measured by AFM after a 20 h anneal at 750 °C, is reduced from 15 nm for 2D buckles to 11 nm for 1D buckles (Fig. 1). To model a_{max}, we turn to strain energy models[10–12] because a highly buckled film should stabilize as it reaches a minimum energy state. The total average strain energy density of a buckled film with a given buckling wavelength λ is

$$\Phi_{\text{total,average}} = \frac{1}{\lambda} \int_0^{\lambda} (\Phi_1 + \Phi_2) dx, \qquad (2)$$

where the two contributions are Φ_1, from the bending of the film and Φ_2, from the in-plane deformation (stretching) of the film. We solve Eq. (2) for arbitrary in-plane stress (after Ref. 10, with $B=0$). The result, where a is the buckling amplitude, is

$$\Phi_{\text{total,average}} = \frac{Eh_{\text{SiGe}}}{(1-\nu^2)} \left(\frac{h_{\text{SiGe}}^2 a^2 k^4}{48} + \frac{3}{64} a^4 k^4 \right)$$
$$+ h_{\text{SiGe}} \left[\frac{1}{2} \sum_{x,y} (\sigma_i \varepsilon_i) + \frac{1}{4} \sigma a^2 k^2 \right]. \qquad (3)$$

The summation is over the two in-plane directions, i.e., it is equal to $2\sigma_{\text{biaxial}}\varepsilon_0$ or $\sigma_{\text{uniaxial}}\varepsilon_0$ for biaxial or uniaxial stress, respectively. In the final term, σ is defined as for Eq. (1). In Fig. 3, the strain energy density is plotted versus buckling amplitude a for the 1D and 2D buckling cases, using the observed buckling wavelengths λ. The curves exhibit minima corresponding to the minimum energy state. The buckling amplitude at this equilibrium point is denoted a_{max}:

$$a_{\text{max}} = \sqrt{-\frac{2}{9} \left[h_{\text{SiGe}}^2 + 3\sigma \left(\frac{1-\nu^2}{E} \right) \left(\frac{\lambda}{\pi} \right)^2 \right]}. \qquad (4)$$

This model predicts smaller buckling amplitudes for 1D versus 2D: $a_{\text{max}}=26$ nm for 2D buckling with $\lambda=0.91$ μm and $a_{\text{max}}=22$ nm for 1D buckling with $\lambda=0.94$ μm. Note that the change in buckling wavelength only accounts for a 1.0 nm shift in a_{max}; the majority of the change in a_{max} is due to the difference between σ_{uniaxial} and σ_{biaxial}. From both modeling and experiment, we have seen that uniaxial stress produces 1D buckles of lower amplitude, compared to 2D buckles (Table I), when the film strain in the direction of buckling is identical in both cases. If $\sigma_{\text{uniaxial}}=\sigma_{\text{biaxial}}$, then τ_B as well as a_{max} will be identical for the uniaxial and biaxial stress cases, while $\Phi_{\text{total,average}}$ will differ by a constant.

For compressively strained SiGe films on BPSG, the 1D buckling process, generated by uniaxial stress, is significantly slower and the buckling amplitude is reduced compared to that for 2D biaxially strained films. This is because buckling in any given direction depends on the film stress in that direction. For the same strain ε_0 in the buckling direction, the Poisson effect causes the uniaxial stress in that direction to be less than the biaxial stress, reducing the driving force for buckling. Technologically, this means that buckling is less of a problem for the creation of uniaxially stressed SiGe and uniaxially strained silicon layers than would be inferred from existing 2D buckling data and models. These results should be valid for other compressively strained films on compliant substrates as well.

[1]K. D. Hobart, F. J. Kub, M. Fatemi, M. E. Twigg, P. E. Thompson, T. S. Kuan, and C. K. Inoki, J. Electron. Mater. **29**, 897 (2000).
[2]H. Yin, R. Huang, K. D. Hobart, Z. Suo, T. S. Kuan, C. K. Inoki, S. R. Shieh, T. S. Duffy, F. J. Kub, and J. C. Sturm, J. Appl. Phys. **91**, 9716 (2002).
[3]H. Yin, K. D. Hobart, R. L. Peterson, S. R. Shieh, T. S. Duffy, and J. C. Sturm, Appl. Phys. Lett. **87**, 061922 (2005).
[4]R. Huang and Z. Suo, Int. J. Solids Struct. **39**, 1791 (2002).
[5]C.-Y. Yu, P.-W. Chen, S.-R. Jan, M.-H. Liao, K.-F. Liao, and C. W. Liu, Appl. Phys. Lett. **86**, 011909 (2005).
[6]W. A. Brantley, J. Appl. Phys. **44**, 534 (1973).
[7]M. Neuberger, *Group IV Semiconducting Materials*, Handbook of Electronic Materials Vol. 5 (IFI/Plenum, New York, 1971).
[8]R. Huang, H. Yin, J. Liang, K. D. Hobart, J. C. Sturm, and Z. Suo, Mater. Res. Soc. Symp. Proc. **695**, 115 (2002).
[9]The uniaxial stress state is confirmed by micro-Raman spectroscopy (see, for example, Refs. 2 and 3).
[10]R. Huang and Z. Suo, J. Appl. Phys. **91**, 1135 (2002).
[11]L. D. Landau and E. M. Lifshitz, *Theory of Elasticity* (Pergamon, London, 1959), pp. 43–60.
[12]S. Timoshenko and S. Woinowsky-Kreiger, *Theory of Plates and Shells*, 2nd ed. (McGraw-Hill, New York, 1959), pp. 366–387.